Journal of Medical Imaging & Case Reports

https://doi.org/10.17756/micr.2024-105

Case Report

Open Access

A Cases Series of Discrepancies in Lung Shunt Fraction Calculation Between 2D Planar and 3D Single Photon Emission Computed Tomography Imaging for Y-90 Radioembolization in Hepatocellular Carcinoma Patients with Ascites

Paula Gamero Kubota, MD, Robert Wagner, MD, Christopher Molvar, MD, James Halama, PhD and Judy R. James, PhD*

Department of Radiology and Medical Imaging, School of Medicine, Loyola University, Maywood, Illinois, United States

***Correspondence to:**
Judy R. James, PhD
Department of Radiology and Medical Imaging,
School of Medicine,
Loyola University,
Maywood, Illinois, United States.
E-mail: judy.james@lumc.edu

Received: May 23, 2024
Accepted: August 01, 2024
Published: August 09, 2024

Citation: Kubota PG, Wagner R, Molvar C, Halama J, James JR. 2024. A Cases Series of Discrepancies in Lung Shunt Fraction Calculation Between 2D Planar and 3D Single Photon Emission Computed Tomography Imaging for Y-90 Radioembolization in Hepatocellular Carcinoma Patients with Ascites. *J Med Imaging Case Rep* 8(1): 18-22.

Published by United Scientific Group

Abstract

Accurate lung shunt fraction (LSF) is essential for safe Yttrium-90 (Y-90) transarterial radioembolization (TARE) treatment of hepatocellular carcinoma (HCC) in patients with ascites. However, traditional 2D imaging might be inaccurate for LSF calculation in this population. This study compared 2D planar imaging with 3D Single photon emission computed tomography (SPECT) for LSF calculation in HCC patients with ascites undergoing TARE. Significant discrepancies were found between 2D and 3D SPECT LSF measurements, suggesting potential overestimation with 2D imaging. 3D SPECT offers a more precise method for LSF calculation in HCC patients with ascites, potentially leading to safer and more effective TARE treatment with higher Y-90 doses.

Keywords

Yttrium-90, Planar imaging, Hepatocellular carcinoma, Ascites, Transarterial radioembolization, Single photon emission computed tomography, Lung shunt fraction

Introduction

HCC is not only common but also a primary complication in patients diagnosed with cirrhosis [1]. Given that ascites is the most common complication of cirrhosis, it's not unusual come across patients who have both HCC and ascites. Among the available treatment modalities, radioactive Y-90 microsphere-based TARE is an effective and well-tolerated option for eligible patients with HCC [2, 3]. Typically, Y-90 is used for unresectable lesions, providing palliation, and delaying disease progression, or for patients who are not liver transplant candidates [4, 5]. Even though there are guidelines for treatment orientation, the ultimate decision-making process relies on the thorough evaluation of individual cases [4].

To ensure the proper administration of Y-90 and avoid complications outside the liver, it is crucial to realize a "mapping" [6] day to weeks in advance. A catheter is guided to the main tumor-feeding artery using fluoroscopy, and technetium-99m (Tc-99m) macro aggregated albumin, is injected for diagnostic purposes. This helps determine tumor size, location, and optimal blood vessels for Y-90 delivery. After a SPECT/CT scan, the interventional radiologist plans the treatment, identifying the best artery for Y-90 administration. It is also used to evaluate the LSF or any unwanted distribution to other organs. LSF indicates the percentage of blood flow from the hepatic artery that goes to the lungs [7]. This measurement is essential in calculating the potential risk of radiation-induced lung issues during Y-90 therapy [4]. Accurate determination of the LSF is necessary to guarantee that the radiation exposure to the lungs remains within safe limits, preventing adverse effects while effectively treating the targeted liver lesion.

Calculating the LSF typically requires using a single 2D anterior and a 2D posterior nuclear medicine (NM) planar imaging. However, the LSF obtained from these 2D images may be inaccurate in cases involving patients with ascites. The presence of ascitic fluid is not visualized on 2D planar images, therefore not considered in the LSF calculation. As a result, the 2D imaging may overestimate the actual LSF, contributing to an artificially high value due to scattered counts from the liver reaching the lungs. Recent literature suggests that alternative methods, such as 3D SPECT on an NM scanner, can provide more precise LSF percentages due to additional scatter and attenuation correction [7-9]. 2D planar imaging produces flat, two-dimensional images with lower spatial resolution; overlapping structures that can obscure details. This is because a collimator that is used to filter gamma rays will only detect those traveling in certain directions. 3D SPECT is obtained with the gamma camera rotating around the patient, and acquiring multiple 2D projections from different angles. 3D image resolution is generally much higher than 2D planar imaging because of the ability to reconstruct 3D information and account for the depth. 3D SPECT imaging also enables superior qunatitave accuracy of radiotracer concentration due to the ability to correct for attenuation, scatter, and detector response variations. More sophisticated scatter correction techniques are used in SPECT to improve image quality and quantitative accuracy. These techniques are less commonly applied in 2D planar imaging. In 3D SPECT, the attenuation of gamma rays as they pass through the body can be corrected using attenuation maps, often obtained from an accompanying CT scan in SPECT/CT systems. This correction is not typically applied in 2D planar imaging. In summary, 3D SPECT LSF estimation will lead to a significant lower misattribution of liver tracer counts to the lungs and results in more accurate count measurement [7]. If an accurate LSF was obtained, the patient would benefit from receiving precise doses of Y-90 ensuring treatment efficacy.

Precise measurement of the LSF is essential to keep the radiation dose to the lungs within safe limits, thereby avoiding adverse effects while delivering an effective therapeutic dose to liver lesions. This careful planning before Y-90 radioembolization significantly lowers the incidence of radiation pneumonitis to less than 1% when lung studies are performed correctly [10].

In this manuscript, we aim to analyze LSF from 3D SPECT images of patients diagnosed with HCC and ascites who underwent Y-90 TARE. The 3D images were processed using Q-volumetrix software on the GE scanner, that combines SPECT and CT from the pre Y-90 images and are background and scatter corrected and recovery co- coefficients applied. Q-volumetrix generated 3D images of the organs with 99mTc-MAA activity in the liver and lungs were clearly visualized. A semi-automatic threshold-based segmentation was performed to outline the liver and the lungs. The LSF, calculated lung dose, and cumulative liver dose were determined using the new 3D imaging for each patient.

This series of cases presents 5 scenarios of a lung shunt discrepancy between planar imaging and SPECT imaging in patients with mild to moderate ascites, as identified from radiological reports. The difference between 2D and 3D SPECT LSF calculations opens a discussion about the accuracy of using planar images in patients with ascites to guide us, addressing not only safety but also the delivered dose and the overall impact on treatment effectiveness.

Case Presentation

Case 1

A 64-year-old woman, with a medical history including hypertension (HTN), dyslipidemia, diabetes mellitus (DM), and nonalcoholic steatohepatitis (NASH) cirrhosis, presented for her routine follow-up examination. Mild ascites was observed during the physical examination, and a CT scan identified a new 2.8 cm lesion in segment 8. Following consultation with an interventional radiologist, Y-90 treatment was recommended.

A SPECT scan was conducted using intravenous Tc-99m MAA to assess the tracer's biodistribution (Figure 1). According to the radiological report, the images revealed a moderate quantity of ascites with a mean Hounsfield co-efficient of 16 in the fluid region of the ascites (Figure 2). Subsequently, LSF calculation was performed using 2D planar imaging, indicating a 5.9% shunt fraction and a lung dose of 2.21. A prescribed dose to the liver of 315 Gy was calculated based on these find-

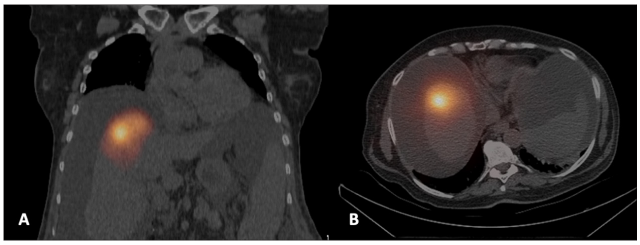

Figure 1: (A) Coronal and **(B)** axial views of a 3D reconstructed and fused SPECT/CT NM pre Y-90 images demonstrating increased Tc-99m uptake in segment 8 of the liver. No other increased uptake was identified in these images.

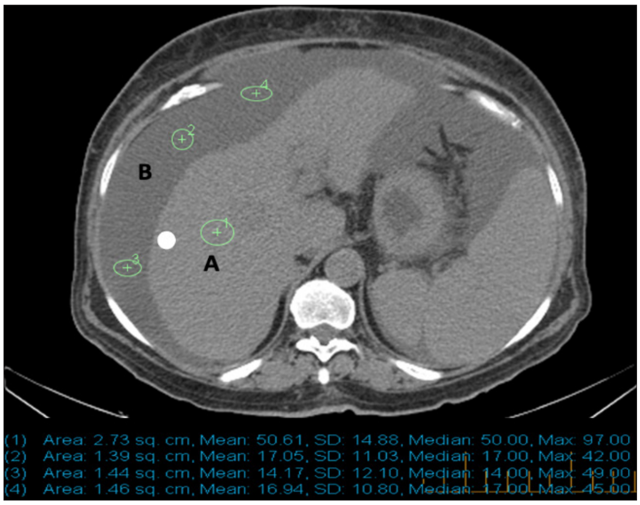

Figure 2: Axial view CT of the abdomen showing moderate free fluid around the liver. **(A)** Hounsfield units mean of the liver 50.61. and **(B)** Hounsfield units mean of the free fluid 16.

ings. 3D SPECT results showed an LSF of 0% and a 0 Gy dose to the lungs (Figure 3 and figure 4). The calculated treatment dose using 3D methodology was 335 Gy.

Case 2

A 60-year-old male with a medical history notable for DM, HTN, alcohol use disorder, and a recent diagnosis of cirrhosis with grade II esophageal varices presents for a follow-up examination. Further evaluation with a CT scan revealed multifocal enhancing lesions surrounding a 9 cm right hepatic cyst, with lesions located within the dome and posterior of the cyst. Additionally, a moderate volume of ascites was observed. Due to the significant tumor burden, the patient was not considered a transplant candidate and was referred to the oncology department. The plan was to proceed with Y-90 therapy.

A SPECT scan, utilizing intravenous Tc-99m MAA, was conducted to evaluate the tracer's biodistribution. The images indicated a moderate quantity of ascites with a mean Hounsfield co-efficient of 6. LSF calculation using 2D planar imaging revealed a 9.9% shunt fraction (Figure 5) and a lung dose of 17.64. A prescribed dose of 152 Gy was calculated based on these findings. In contrast, 3D SPECT results showed an LSF of 4% and a lung dose of 7.13 Gy. The calculated treatment dose using 3D methodology was 161 Gy.

Case 3

A 67-year-old male with a history of HTA, obstructive sleep apnea, and NASH cirrhosis, complicated by a 3.2 x 2.8 cm lesion on the right posterior lobe. The patient underwent a previous evaluation for a liver transplant, but it was declined due to preserved liver function. Y-90 therapy was recommended. He has undergone previous evaluation for a liver transplant, but it was declined due to preserved liver function. Y-90 therapy was recommended. The LSF calculated with 2D planar imaging is 1.6%, dose to the lungs 0.78 Gy and liver dose 421 Gy. while using 3D SPECT imaging the LSF was is 0%, dose to the lungs 0 Gy and liver dose 426 Gy.

Case 4

A 65-year-old male with a history of hepatitis C-related cirrhosis, complicated with HCC and elevated alpha-fetoprotein, and a history of Y-90 procedures in 2022 and 2023, presents for follow-up. The recent CT scan indicates disease progression with the presence of several new lesions and an increase in size compared to prior scans. A chest CT and bone scan reveal no signs of metastatic disease, but imaging detects a mild amount of ascites (mean Hounsfield co-efficient of 12.5 units). Aggressive Y-90 treatment for his residual small lesions was recommended. Subsequent SPECT images with intravenous Tc-99m MAA showed the presence of ascites with a mean of 12 Hounsfield units. The LSF, calculated using 2D planar imaging, was 1.8%, with a lung dose of 2.9 Gy and a cumulative dose to the lungs of 21.87 Gy. The liver dose calculated was 137 Gy. In contrast, 3D SPECT imaging showed an LSF of 0%, with no lung dose (0 Gy), a cumulative dose to the lungs of 18.97 Gy, and a liver dose of 139 Gy.

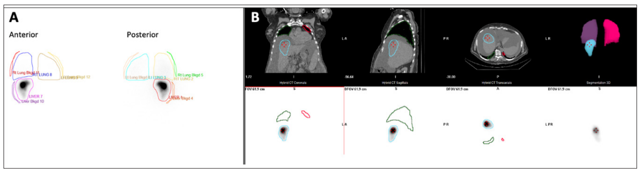

Figure 3: (A) Showing 2D planner LSF imaging compared to **(B)** showing 3D SPECT LSF imaging for the same patient.

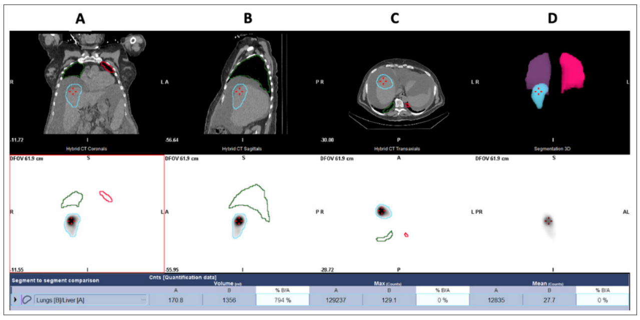

Figure 4: Top row showing: **(A)** coronal, **(B)** sagittal, and **(C)** axial CT views generated by Q-volumetric using 3D SPECT images with clear visualization of the Tc-99m MAA activity and uptake in the liver and spill out also out into the lung regions. SPECT LSF was 0%.

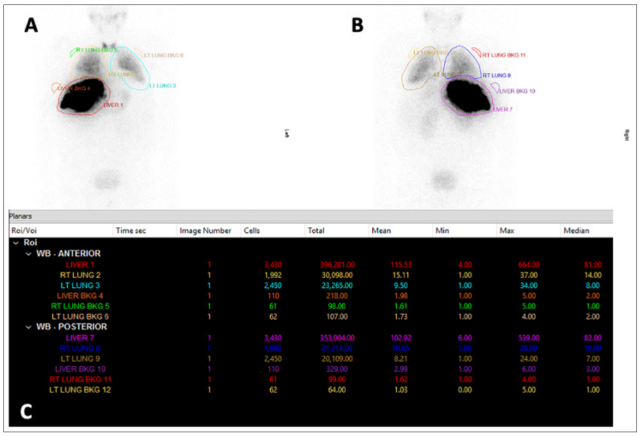

Figure 5: (A) Anterior, **(B)** posterior 2D planar views showing delineated liver and lung regions, and **(C)** counts using coronal slices from Tc-99m MAA planer imaging for the calculation of LSF. The planar LSF was 9.9%.

Case 5

A 78-year-old female patient with a history of NASH-related cirrhosis presents with a lesion spanning segments 5 and 6 in the right lobe, measuring at least 4.7 x 5.6 cm. The lesion appears predominantly hypointense on precontrast imaging and exhibits homogeneous early enhancement on early postcontrast phases, with early washout on portal venous phases. Additionally, ascites was noted on MRI. The recommended course of action was Y-90 treatment.

During the LSF assessment mapping, mild ascites was also observed on SPECT (Figure 6) The LSF, calculated using 2D planar imaging, was determined to be 17.2%. Based on these higher LSF results, the patient was determined unsuitable for treatment, and no further calculations were made. However, using 3D SPECT imaging yielded an LSF of 6% (Figure 7), making the patient eligible for treatment.

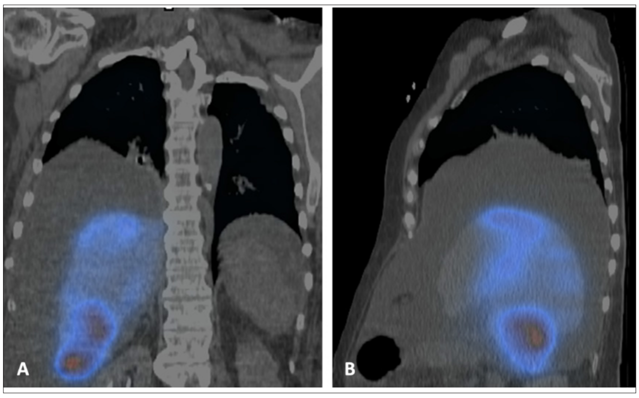

Figure 6: **(A)** Coronal, and **(B)** sagittal views of a 3D reconstructed and fused SPECT/CT NM pre Y-90 images demonstrating most of the tracer deposited within the liver right lobe. No abnormal localization of tracer was noted outside the liver.

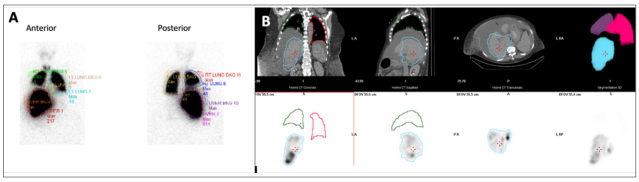

Figure 7: **(A)** Showing 2D planar LSF imaging compared to **(B)** showing 3D showing 3D SPECT LSF imaging for the same patient.

Discussion

The cases presented highlight the differences between 2D planar and 3D SPECT results in LSF calculation in the scenario of ascites. Notably, four cases exhibited a 0% LSF, and one case showed less than half of the original 2D LSF. Although there are no previous studies on LSF methods in patients with ascites, these results align with findings from Struycken et al. [11] whose studies indicated a mean LSF of 25.1% with 2D imaging and 16% using SPECT methods. Recently, Lee et al. [12] also reported similar results this year, with 9.8% and 5.6% for 2D and 3D imaging, respectively.

Dittman et al. studied 50 patients and calculated the LSF from 2D planar imaging, which showed a median of 6.8%, while SPECT/CT revealed a median of 1.9%. Based on 2D planar imaging, dose reduction or contraindications for radiotherapy had to be considered in 10 patients, as their LSF was 10% or higher. In contrast, SPECT/CT quantification indicated significant shunting in only 2 patients [13]. These findings suggest that using SPECT for LSF calculation could prevent unnecessary dose reductions.

Furthermore, the clinical relevance of having a more precise LSF and avoiding overestimation is that a more accurate dosage of Y-90 can be delivered during treatment, often resulting in a higher dose. As evidenced by the cases presented, all of them experienced an increase in the administered dose. Lam et al. [2] determined that higher doses are associated with a significant probability of achieving objective responses and improved overall survival. These results are supported by the study conducted by Moon et al. [13], which identified lower doses of treatment as a risk factor for HCC recurrence.

Although the calculated LSF and the radiation dose to the liver increases between 2D and 3D SPECT methods, the impact on the dose to the lungs was minimal, with one exception. This opens a new topic of research for prioritizing cases where the LSF is crucial, or cases where it may be considered optional due to the minimal dose passing to the lungs. Each case of HCC treated with pre Y-90 should undergo personalized evaluation and management, considering the main goals, quality of life, available options, and patient preferences. LSF calculation should not be an exception.

Conclusion

The discrepancies between 2D planar and 3D SPECT imaging, highlighted in our case series, underscore the necessity for precision in LSF calculations, especially in cases involving patients with ascites. Although the impact on lung dose remains minimal, these findings contribute to the considerations in treatment planning and enhancing patient's outcomes and reduced need for repeat imaging.

Acknowledgments

The authors would like to thanks Mr. Ryan D Thomas for his valuable assistance in preparing the manuscript.

Conflicts of Interest

None.

References

1. Premkumar M, Anand AC. 2022. Overview of complications in cirrhosis. *J Clin Exp Hepatol* 12(4): 1150-1174. https://doi.org/10.1016/j.jceh.2022.04.021
2. Lam M, Garin E, Maccauro M, Kappadath SC, Sze DY, et al. 2022. A global evaluation of advanced dosimetry in transarterial radioembolization of hepatocellular carcinoma with yttrium-90: the TARGET study. Eur J Nucl Med Mol Imaging 49(10): 3340-3352. https://doi.org/10.1007/s00259-022-05774-0
3. Lau WY, Kennedy AS, Kim YH, Lai HK, Lee RC, et al. 2012. Patient selection and activity planning guide for selective internal radiotherapy with yttrium-90 resin microspheres. Int J Radiat Oncol Biol Phys 82(1): 401-407. https://doi.org/10.1016/j.ijrobp.2010.08.015
4. Salem R, Padia SA, Lam M, Chiesa C, Haste P, et al. 2023. Clinical, dosimetric, and reporting considerations for Y-90 glass microspheres in hepatocellular carcinoma: updated 2022 recommendations from an international multidisciplinary working group. Eur J Nucl Med Mol Imaging 50(2): 328-343. https://doi.org/10.1007/s00259-022-05956-w
5. Garg T, Shrigiriwar A, Habibollahi P, Cristescu M, Liddell RP, et al. 2022. Intraarterial therapies for the management of hepatocellular carcinoma. *Cancers* 14(14): 3351. https://doi.org/10.3390/cancers14143351
6. Mikell JK, Dewaraja YK, Owen D. 2020. Transarterial radioembolization for hepatocellular carcinoma and hepatic metastases: clinical aspects and dosimetry models. Semin Radiat Oncol 30(1): 68-76. https://doi.org/10.1016/j.semradonc.2019.08.005
7. Torkian P, Ragulojan R, J. Woodhead G, D'souza D, Flanagan S, et al. 2022. Lung shunt fraction quantification methods in radioembolization: what you need to know. Br J Radiol 95(1139): 1-5. https://doi.org/10.1259/bjr.20220470
8. Braat AJ, Smits ML, Braat MN, van den Hoven AF, Prince JF, et al. 2015. ^{90}Y hepatic radioembolization: an update on current practice and recent developments. *J Nucl Med* 56(7): 1079-1087. https://doi.org/10.2967/jnumed.115.157446

9. Allred JD, Niedbala J, Mikell JK, Owen D, Frey KA, et al. 2018. The value of ^{99m}Tc-MAA SPECT/CT for lung shunt estimation in ^{90}Y radioembolization: a phantom and patient study. EJNMMI Res 8(1): 1-12. https://doi.org/10.1186/s13550-018-0402-8

10. Spina JC, Hume I, Pelaez A, Peralta O, Quadrelli M, et al. 2019. Expected and unexpected imaging findings after ^{90}Y transarterial radioembolization for liver tumors. Radiographics 39(2): 578-595. https://doi.org/10.1148/rg.2019180095

11. Struycken L, Patel M, Kuo P, Hennemeyer C, Woodhead G, et al. 2022. Clinical and dosimetric implications of calculating lung shunt fraction for hepatic ^{90}Y radioembolization using SPECT/CT versus planar scintigraphy. *Am J Roentgenol* 218(4): 728-737. https://doi.org/10.2214/ajr.21.26663

12. Lee JH, Lee CH, Kim M, Song YS, Yoon CJ, et al. 2023. CT texture features and lung shunt fraction measured using ^{99m}Tc-macroaggregated albumin SPECT/CT before trans-arterial radioembolization for hepatocellular carcinoma patients. *Sci Rep* 13(1): 1-9. https://doi.org/10.1038/s41598-023-49787-7

13. Moon S, Kim GM, Won JY, Kwon JH, Park J, et al. 2024. Clinical course of patients with hepatocellular carcinoma who experienced radiologic complete response after radioembolization. Front Oncol 14: 1-8. https://doi.org/10.3389/fonc.2024.1349632